JACS Au
AN OPEN ACCESS JOURNAL OF THE AMERICAN CHEMICAL SOCIETY

pubs.acs.org/jacsau
Article

Development of a Fluorescently Labeled Ligand for Rapid Detection of DAT in Human and Mouse Peripheral Blood Monocytes

Gisela Andrea Camacho-Hernandez, Adithya Gopinath, Amarachi V. Okorom, Habibeh Khoshbouei, and Amy Hauck Newman*

Cite This: *JACS Au* 2024, 4, 657−665
Read Online

ACCESS | Metrics & More | Article Recommendations | Supporting Information

ABSTRACT: The dopamine transporter (DAT) is one of the key regulators of dopamine (DA) signaling in the central nervous system (CNS) and in the periphery. Recent reports in a model of Parkinson's disease (PD) have shown that dopamine neuronal loss in the CNS impacts the expression of DAT in peripheral immune cells. The mechanism underlying this connection is still unclear but could be illuminated with sensitive and high-throughput detection of DAT-expressing immune cells in the circulation. Herein, we have developed fluorescently labeled ligands (FLL) that bind to surface-expressing DAT with high affinity and selectivity. The diSulfoCy5-FLL (**GC04-38**) was utilized to label DAT in human and mouse peripheral blood mononuclear cells (PBMCs) that were analyzed via flow cytometry. Selective labeling was validated using DAT KO mouse PBMCs. Our studies provide an efficient and highly sensitive method using this novel DAT-selective FLL to advance our fundamental understanding of DAT expression and activity in PBMCs in health and disease and as a potential peripheral biomarker.

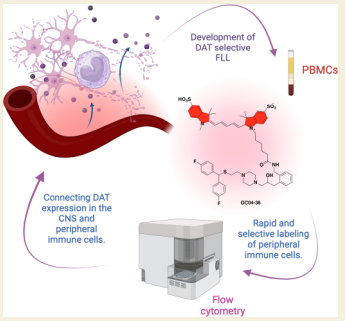

KEYWORDS: *dopamine transporter, PBMC, flow cytometry, fluorescent probes, fluorescently labeled ligands*

INTRODUCTION

Altered dopamine signaling in the central nervous system (CNS) has been the subject of many studies, as it has become a fundamental feature of numerous CNS diseases and disorders.[1] In Parkinson's disease (PD), recent reports have found that this dysregulation is not limited to the CNS, as it is present in the periphery, affecting peripheral immunity. The dopamine transporter (DAT)[2,3] serves as a pivotal connector to these two key features in PD: inflammation and altered dopamine signaling. In the CNS, this member of the reuptake-1 monoamine transporters (MATs) clears extracellular dopamine by transporting it into the cell for storage in vesicles.[4,5] Recent studies have shown that peripheral immune cells such as monocytes and macrophages express DAT and norepinephrine transporter (NET). The bidirectional communication between the CNS and the peripheral immune system is a well-established concept showing changes in dopamine levels in the CNS, and the activity of dopamine neurons regulates peripheral immune responses.[6−11] Since many peripheral immune cells express DAT, by directly influencing DAT-expressing peripheral immune cells and thus peripheral immunity, DAT ligands can trigger a feed-forward cascade that impacts the bidirectional communication between the CNS and peripheral immune systems.[12] For example, in PD DAT, a classic CNS biomarker is increased in peripheral blood mononuclear cells (PBMCs) of drug-naïve PD patients, whereas there is a decrease of this protein in the CNS.[9] While there is a clear connection between dopamine neuronal loss and increased DAT expression in peripheral immune cells in PD, the mechanism by which this occurs is still unclear. Developing new methodologies and tools to facilitate elucidating these relationships and the mechanisms underlying them may facilitate alternative strategies to prevent, treat, and/or diagnose PD.

Fluorescently labeled ligands (FLL) have proven highly useful as tools to study protein expression, localization, distribution, and downstream processes in distinct live cell systems, opening a venue to study endogenously expressed proteins.[13−16] Elements that traditionally constitute the structure of these probes are (1) the parent ligand, which acts as the "carrier" of the probe and binds to the target; (2) the fluorescent dye, which varies depending on the application of the FLL; and (3) the linker, which tethers these two elements together.[17,18]

We have previously reported several FLL to study MATs such as JHC1-064, a rhodamine-labeled fluorescent cocaine-based analogue, which has been extensively used due to its high binding affinity, slow off-rate, and lack of selectivity for all three members of this transporter family.[13,18,19] More recently, analogues of JHC1-064, DG3-80, and DG4-91 that used Janelia Fluorophores (JF549 and JF646, respectively) with a modified polyethylene glycol tether proved useful for single-particle tracking and dSTORM experiments.[15,20] In addition, we have

Received: November 16, 2023
Revised: January 5, 2024
Accepted: January 8, 2024
Published: January 24, 2024

https://doi.org/10.1021/jacsau.3c00719
JACS Au 2024, 4, 657−665

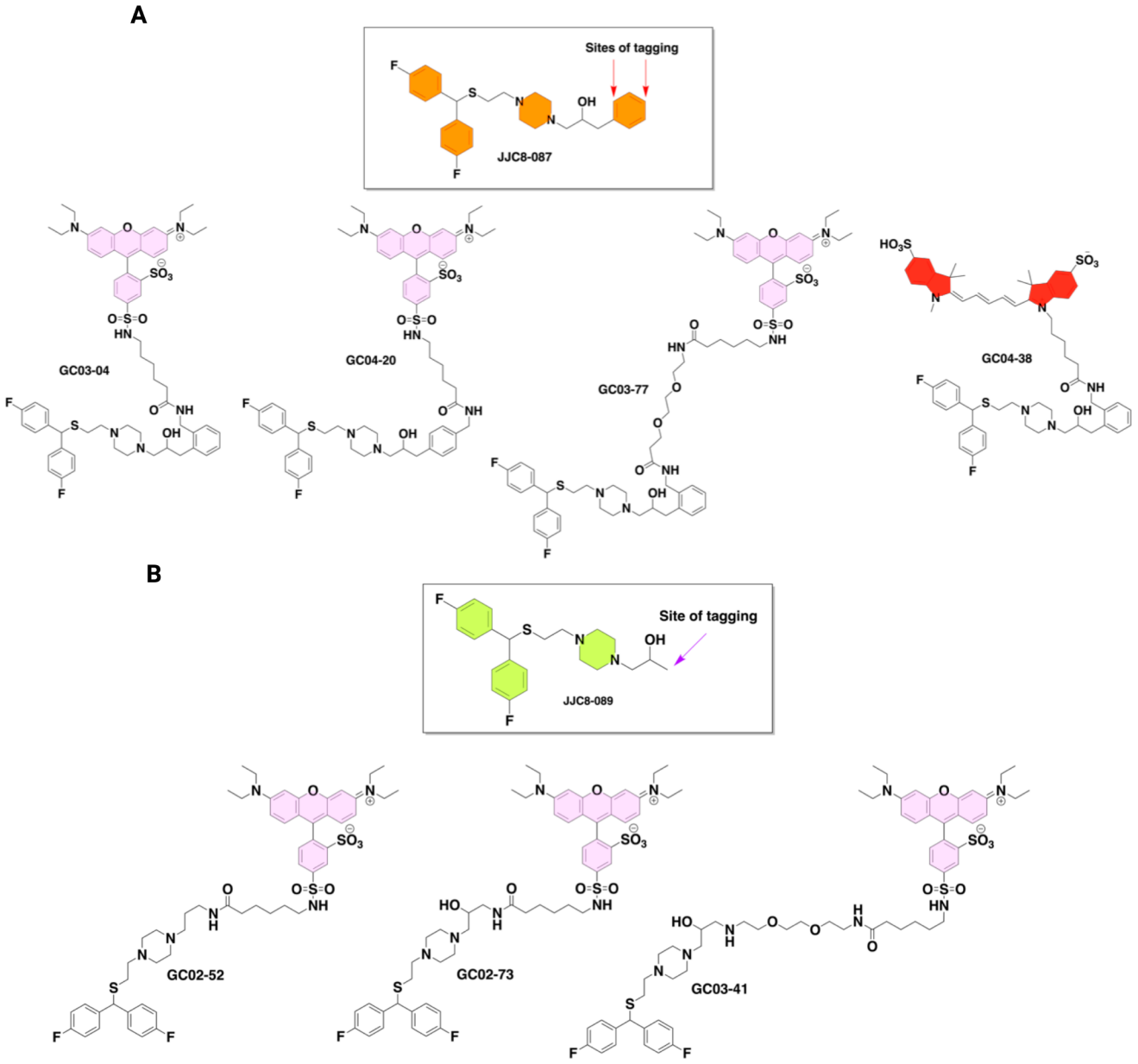

Figure 1. Rational design and synthesis of DAT-selective FLL. (A) JJC8-087 and FLL analogues. (B) JJC8-089 and FLL analogues.

expanded our fluorescent tool box by generating other MAT-selective FLL, such as VK2-83,[21] a selective serotonin transporter (SERT) FLL based on (S)-citalopram, and more recently AC1-146,[22,23] a nisoxetine-based NET preferential probe.

Herein, we describe the design and synthesis of a library of DAT-selective FLL, utilizing the atypical DAT inhibitors JJC8-087 and JJC8-089 (Figure 1A,B) as parent ligands.[24] Based on the membrane-impermeant diSulfoCy5 fluorophore and its DAT-selective binding profile, **GC04-38** was selected to label DAT in monocytes freshly isolated from mouse and human blood samples. Using a modification of the previously published flow cytometry method,[25] we validated the selective labeling of DAT by GC04-38. Furthermore, by replacing the use of a DAT antibody for this FLL, we substantially reduced the sample preparation time from 165 to only 30 min. In summary, our findings indicate that this fluorescently labeled ligand, GC04–38, is highly useful for investigating DAT activity and its functions on immune cells. While recent data on immune cell characterization support the idea that immune cells expressing DAT could serve as a supplementary diagnostic tool for PD and reliably detect methamphetamine-induced disruptions in the peripheral immune system, **GC04–38** offers a noninvasive, high-throughput method for detecting these DAT-expressing immune cells in the bloodstream. This makes it particularly valuable for studying CNS-to-peripheral DAT regulatory mechanisms in other neurological and neuropsychiatric conditions, such as ADHD across various species.

RESULTS AND DISCUSSION

Design, Synthesis, and Binding Affinities of DAT-Selective Fluorescently Labeled Ligands

The syntheses of a series of novel FLL are described in detail in the Supporting Information. For our design, we started with two high-affinity atypical and DAT-selective inhibitors, JJC8-087 and JJC8-089 (Figure 1A,B)[24] as parent ligands. Binding

https://doi.org/10.1021/jacsau.3c00719
JACS Au 2024, 4, 657–665

Table 1. Binding Affinities of the Novel DAT FLL

	$K_i \pm$ SEM (nM)[a] [n]					
compound	rDAT	rSERT	rNET	hDAT	rSERT/rDAT	rNET/rDAT
JJC8-087[b]	6.72 ± 0.977	1770 ± 234	>10,000	1.19 ± 0.110 [3]	263	>1488
JJC8-089[b]	16.7 ± 1.22	213 ± 13.2	1950 ± 227	N.T.	13	117
GC02-52	448 ± 76.0 [5]	6660 ± 668 [3]	>10,000	N.T.	15	>22
GC02-73	406 ± 54.3 [3]	3320 ± 151 [3]	>10,000	N.T.	8	>25
GC03-04	140 ± 22.5 [3]	2920 ± 194 [3]	>10,000	N.T.	21	>70
GC03-41	236 ± 25.0 [3]	1130 ± 187 [3]	1700 ± 165 [3]	N.T.	5	7
GC03-77	373 ± 88.4 [4]	5220 ± 293 [4]	8200 ± 730 [3]	N.T.	14	22
GC04-20	219 ± 27.2 [3]	5910 ± 2030 [3]	>10,000	N.T.	27	>46
GC04-38	159 ± 15.7 [3]	4410 ± 822 [3]	>10,000	191 ± 16.5 [3]	28	>63

[a]Each K_i value represents data from at least three independent experiments, each performed in triplicate. K_i values were obtained utilizing GraphPad Prism. Binding assay procedures are described in detail in the Experimental Methods (SI). [n] = number of experiments. N.T. = not tested. [b]Values of JJC8-087 and JJC8-089 were previously reported in Cao et al.[24] and are included for comparison.

affinities (Table 1) for rDAT, rSERT, and rNET of all final compounds were obtained via the radioligand binding assay in Sprague−Dawley rat brain membranes using methods previously described and compared to the parent ligands.[26] Fluorescence labeling of the parent ligands was chosen based on previously reported structure−activity relationship studies, where additional structural modifications were predicted to only modestly compromise DAT binding affinities.[24] Of note, the fluorophores are structurally large and sometimes charged or are lipophilic molecules that must be tethered to the parent ligand in an optimal distance.

Moreover, careful choice of where on the drug molecule the tether is appended is also critical for the success of identifying a high-affinity FLL. In addition, it is likely that as in other systems (e.g., chemigenetic indicators),[27] the fluorescent dye may interact with residues outside the binding pocket, affecting protein conformation and potentially promoting distinct interactions that will ultimately influence the binding nature of the probe. In this study, two sites of tagging were explored in JJC8-087 (Figure 1B), where the ortho-substituted **GC03-04** (rDAT K_i = 140 nM) analogue had the highest rDAT binding affinity of all the compounds synthesized in the series and shared similar rDAT binding affinity with the para-substituted **GC04-20** probe (K_i = 219 nM).

Both compounds had similar SERT and NET selectivity profiles, having more than 20-fold selectivity with respect to SERT and no interaction with NET at 10 μM (Table 1). Increasing the linker length with a PEG2 (ethylene glycol) linker between the parent ligand and the fluorescent dye as depicted in **GC03-77** resulted in a slight decrease in rDAT affinity (rDAT K_i = 373 nM) and a decrease in selectivity with respect to SERT and NET. Replacing the Rhodamine Red fluorescent dye in **GC03-04** with DiSulfoCy5 afforded **GC04-38** with a suitable rDAT binding profile (rDAT K_i = 159 nM) and selectivity with respect to SERT (28-fold) and NET (63-fold), suggesting versatility when the fluorescent dye is exchanged. Analogues based on JJC8-089 were labeled as depicted in Figure 1C, where the fluorescent tag was placed on the terminal 2-O*H*-propyl moiety, affording three novel ligands **GC02-52**, **GC02-73**, and **GC03-41** with moderate binding affinities for rDAT (K_i = 236−448 nM) and low to moderate selectivity with respect to SERT or NET. Similar to **GC03-77**, increasing the linker length with a PEG2 linker between the parent ligand and the fluorescent dye afforded lower DAT over SERT or NET selectivity (Table 1). Overall, compounds based on JJC8-87, as predicted by the parent ligand (Figure 1B and Table 1), had the higher rDAT binding affinities and selectivities over SERT and NET. Lastly, compound **GC04-38**, was further assessed in hDAT utilizing cell membranes from a stable HEK293-hDAT cell line (Table 1). Despite the change of species, DAT binding affinity was retained (K_i = 191 nM) when compared to that of rDAT (K_i = 159 nM).

GC04-38-Bound DAT Is Reliably Detectable via Flow Cytometry

DAT is expressed on human and murine immune cells,[9−12,25,28,29] is functional,[12] and is detected via immunostaining, confocal microscopy,[12] and flow cytometry[9,25] using the MAB369 antibody against the N-terminus of DAT.[30] To our knowledge, conventional flow cytometry is the most used high-throughput assay to identify DAT-expressing immune cells in blood circulation. The availability of the fluorescent ligand that specifically targets membrane DAT would shorten sample preparation by eliminating multiple steps including permeabilization, incubations with primary and secondary antibodies, and washes in between. Existing DAT FLL such as JHC1-064 have a few insurmountable problems, including cross reactivity with other MATs and low detectability via flow cytometry (Supplementary Figure S1). Therefore, we first investigated the efficacy, specificity, and utility of flow cytometry for **GC04-38** in detecting DAT in hDAT-YFP-expressing HEK cells, a reduced model system used to study DAT biology. To emulate a suspension of DAT-expressing immune cells in circulation, we did not incubate the adhering hDAT-YFP-expressing HEK cells with **GC04-38**; instead, the cells were lifted, suspended, and incubated with **GC04-38** for 30 min and assessed via flow cytometry for colocalization of the **GC04-38** fluorescent signal

https://doi.org/10.1021/jacsau.3c00719
JACS Au 2024, 4, 657−665

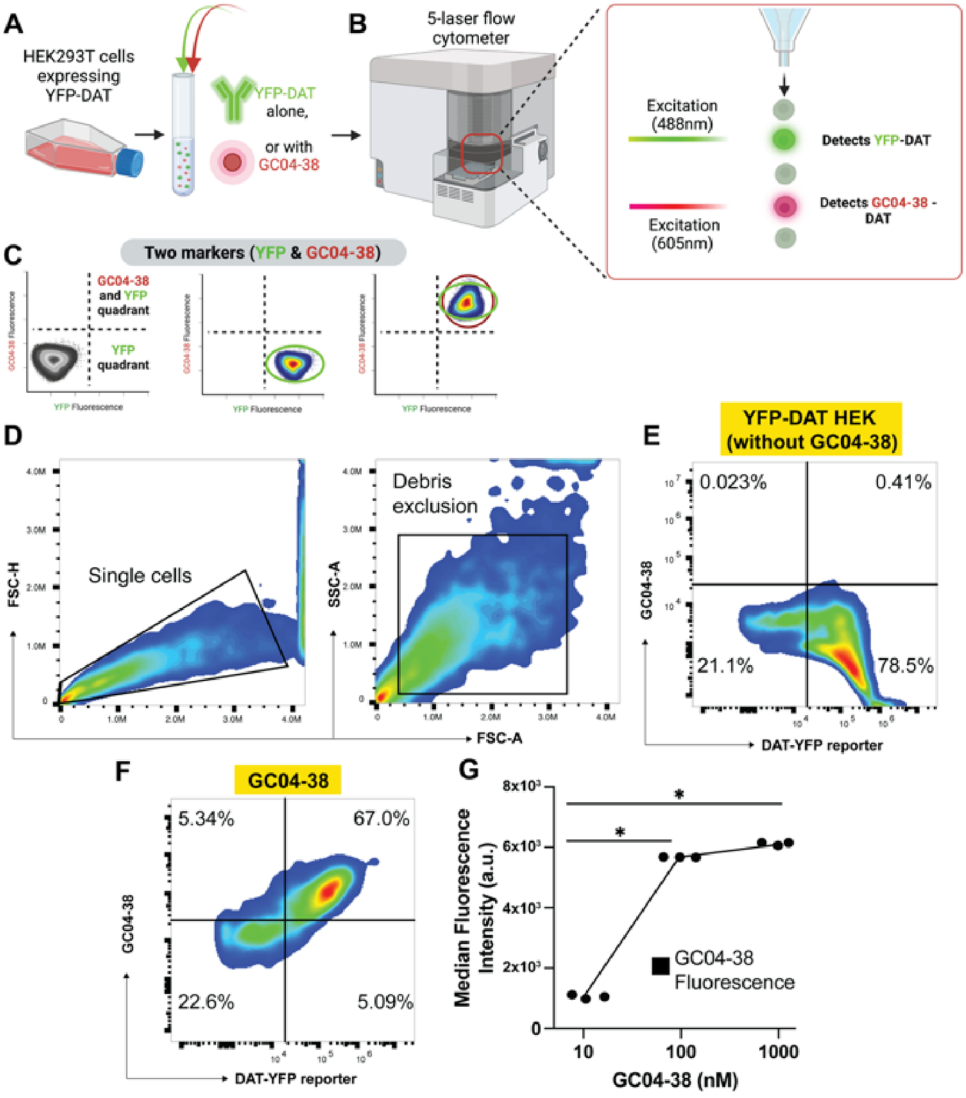

Figure 2. GC04-38 reliably detects DAT in YFP-DAT-expressing HEK293T cells. (A) Schematic representation of the flow cytometry experimental design. HEK293T cells expressing YFP-DAT were assessed via flow cytometry for expression of YFP, and the colocalization of the YFP signal with **GC04-38**. The YFP reporter is bound to the intracellular domain of DAT, whereas **GC04-38** binds to the extracellular DAT domain. (**B**) YFP-expressing and **GC04-38**-bound cells pass through lasers in series, each laser exciting a fluorophore of interest (i.e., YFP or **GC04-38**). The fluorescent emission(s) are detected and identified according to their excitation/emission profile. (C) YFP and **GC04-38** signals were assessed by plotting YFP on the *X*-axis, and **GC04-38** on the *Y*-axis. YFP was detected via fluorescence in the YFP channel in the lower right quadrant (visualized as a rightward shift in the cells of interest) whereas **GC04-38** fluorescence was detected via fluorescence in the red channel (indicated by the cells of interest shifting upward on the *Y*-axis). Cells positive for both markers are seen in the upper right quadrant (C, far right, red and green circles). (D) Shows gating single cells and excluding debris. (E) The YFP signal in the absence of **GC04-38** is detected in the lower-right quadrant; non-YFP-expressing cells are detected in the lower-left quadrant. (F) Cells treated with **GC04-38** (100 nM) for 30 min at room temperature showed colocalization of the YFP signal with **GC04-38** detected in the upper-right quadrant. Similar to (B), the non-YFP-expressing cell population detected in the lower-left quadrant. (G) Dose−response for **GC04-38** treatments of YFP-DAT cells suggest that **GC04-38** saturates available DAT at 100 nM, with no appreciable signal increase with higher concentrations of **GC04-38**. Fluorescence is shown on the *Y*-axis as median fluorescence intensity (arbitrary units, a.u.) ($n = 3$ independent replicates per group; one-way ANOVA with Tukey's post hoc (F (2,6) = 1658, $p < 0.0001$), *$p < 0.0001$). Individual data points are included to show spread. Note: quadrants shown in (C) and (E−G), are only used when assessing colocalization of two markers as a rightward or upward shift in the same sample.

with the YFP-DAT fluorescent signal (Figure 2A−C). In the five-laser flow cytometry system used in this study, YFP and **GC04-38** are excited by separate lasers and detected by separate detectors, allowing detection of colocalized signals with high specificity. After gating for single cells and excluding debris (Figure 2D), gates were set to accurately identify the YFP signal independent of the **GC04-38** signal (Figure 2E, lower-right quadrant). YFP-DAT colocalization with **GC04-38**-tagged cells indicates specificity of **GC04-38** for hDAT tagged with YFP (Figure 2F). A dose−response assay revealed a saturable signal, where 100 nM **GC04-38** produced maximum staining for YFP-DAT HEK293 cells, consistent with the finite number of membranes hDATs that can bind to **GC04-38** (Figure 2G). The results suggest that **GC04-38** bound DAT can be detected via a flow cytometry assay, producing a specific signal in a reduced model system expressing DAT.

https://doi.org/10.1021/jacsau.3c00719
JACS Au 2024, 4, 657−665

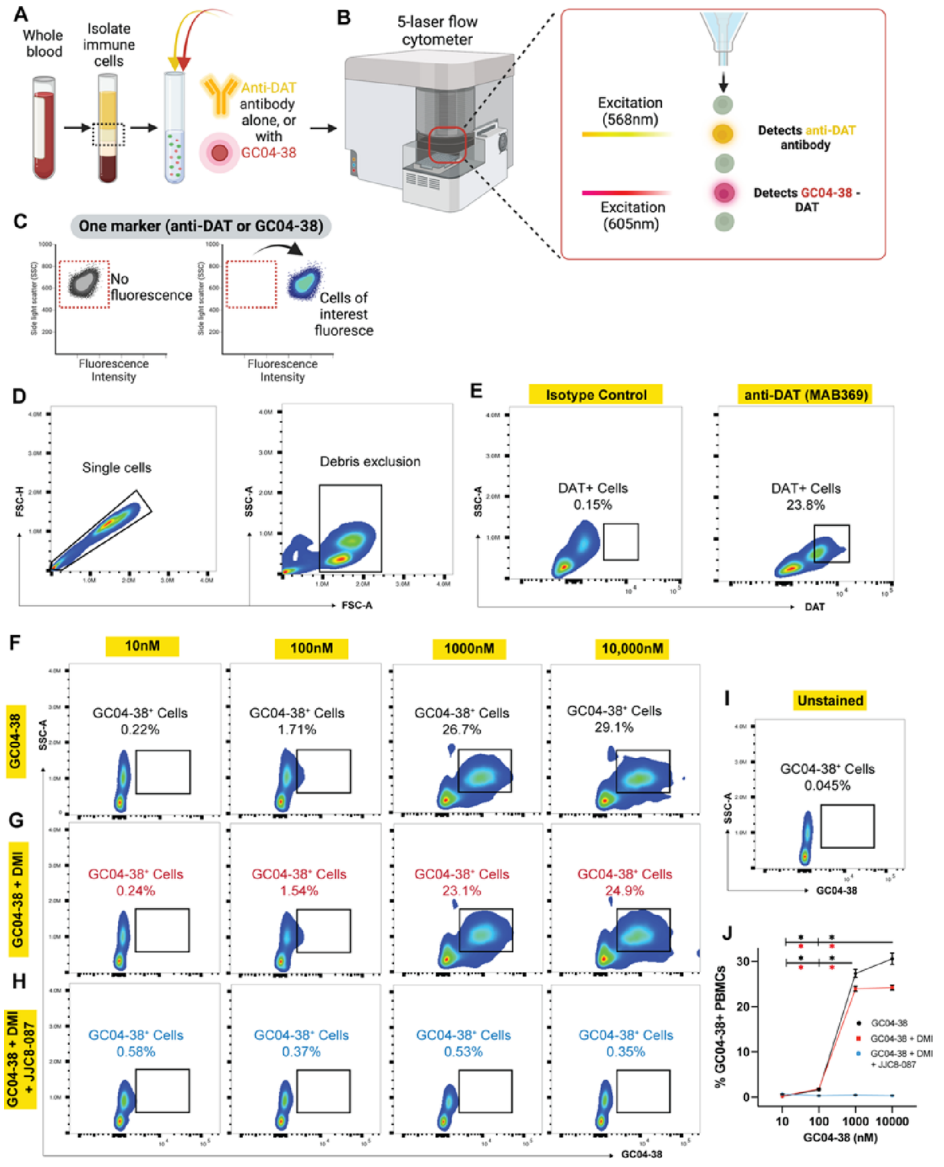

Figure 3. GC04-38 reliably detects DAT on human circulating peripheral blood monocytes (PBMCs). Schematic representation of flow cytometry experimental design (A–C). (A) PBMCs were isolated from whole blood via density media centrifugation treated with **GC04-38** (bound to the extracellular DAT domain) or antibody stained with anti-DAT antibody (MAB369 bound to the intracellular DAT domain). (B) Samples were analyzed via flow cytometry on a five-laser Cytek Aurora Spectral Cytometer. Antibody-bound and **GC04-38**-bound cells pass through lasers in series, each laser exciting a fluorophore of interest (i.e., YFP or **GC04-38**). The fluorescent emission(s) are detected and identified according to their excitation/emission profile. (C) Immunostaining with anti-DAT antibody followed by flow cytometry detection complemented **GC04-38**-bound DAT. Samples stained with *either* anti-DAT antibody *or* **GC04-38** were visualized in freshly isolated human PBMCs. (D) The cells were gated for single cells and debris exclusion. (E) Depicts specific staining for DAT+ monocytes and minimal background signal.[12,25] (F–J) **GC04-38** treatment produced an increasing fluorescent signal in a dose-dependent manner (10, 100, and 1000 nM) relative to the unstained negative control (D). At 1000 nM **GC04-38**, the percentage of DAT-bound **GC04-38** is comparable to immunostaining shown in (G); at 10,000 nM, the DAT signal is saturated. (G) Consistent with our previous data,[9,12] a small percentage of human PBMCs express norepinephrine transporter (NET); consistently, pretreatment with DMI slightly reduced the signal. (H) Pretreatment with nonfluorescent JJC8-087, the parent compound for **GC04-38**, at 100 μM abolished the fluorescent signal from **GC04-38**. (J) The **GC04-38** fluorescent signal (black), the signal in the presence of DMI (red), and the signal when samples are preincubated with nonfluorescent JJC8-087 (blue) (n = 3 independent replicates per group; one-way ANOVA with Tukey's post hoc (**GC04-38**: $F(3,8) = 446.7$; **GC04-38**+DMI: $F(3,8) = 1168$; **GC04-38**+DMI+JJC8-087: $F(3,8) = 22.39$); *$p < 0.0001$). Data are shown as the mean ± SEM.

GC04-38 Detects DAT on Human PBMCs with a High Degree of Specificity and Detectability via the Flow Cytometry Assay

Prior studies employed anti-DAT antibody staining followed by flow cytometric analysis[9−11] to detect DAT-expressing immune cells in the peripheral circulation. MAB369 is a widely used primary antibody that effectively and reproducibly recognizes the intracellular N-terminal domain of DAT in permeabilized preparations. Therefore, we compared the specificity of MAB369 and **GC04-38** in identifying DAT-expressing PBMCs in human samples (Figure 3A–C). Human PBMCs were either subjected to the multistep protocol including permeabilization, incubations with anti-DAT antibody, and incubation with species-specific fluorescent secondary antibody and washes in between (Figure 3E), or they were subjected to the single step protocol of **GC04-38** incubation (10, 100, 1000,

https://doi.org/10.1021/jacsau.3c00719
JACS Au 2024, 4, 657−665

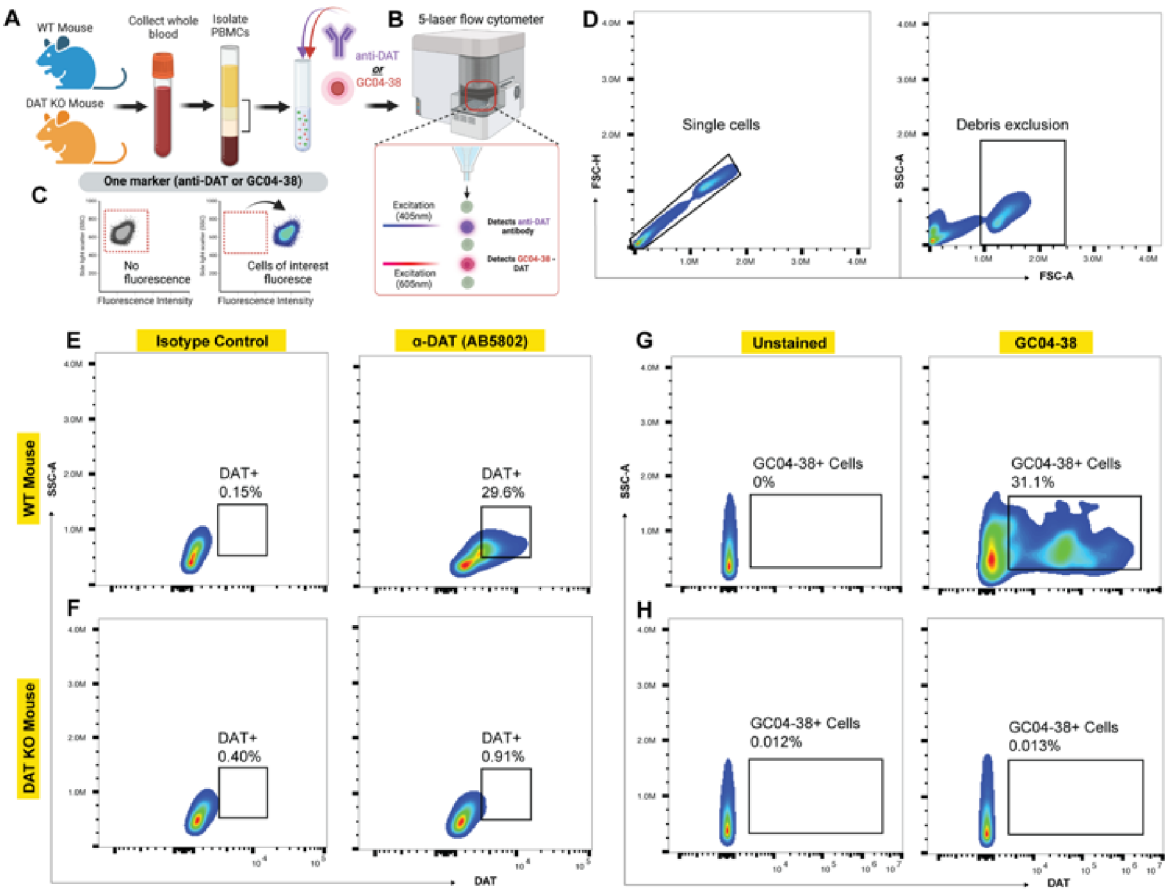

Figure 4. Flow cytometry detection of **GC04-38**-bound DAT on circulating peripheral blood monocytes (PBMCs) is specific. (A) PBMCs isolated from whole blood obtained from mice with genetic DAT deletion (DAT KO) and wild-type control (WT) were treated with either anti-DAT antibody (AB5802) or treated with **GC04-38** for 30 min at room temperature and then (B) assessed via flow cytometry. (C) Increased fluorescence intensity indicates a signal from cells of interest. (D) As described in Figures 1−3, single cells were isolated and then gated to exclude debris. (B) In the absence of DAT antibody, no signal is detected, i.e., "Isotype control". (E) In WT mice, DAT antibody reliably detects DAT on PBMCs, which is consistent with a previous report showing that ∼30% of mouse PBMCs express DAT.[9] (F) No staining is observed in $DAT^{-/-}$. (G) Treatment of WT mouse PBMCs with **GC04-38** results in a robust DAT signal (right panel) relative to unstained control (left panel) consistent with the obtained anti-DAT antibody shown in (E). (H) **GC04-38** produces no signal in DAT KO mice, indicating **GC04-38** detection of DAT on PBMCs is specific. Data shown are representative of $n = 3$ independent replicates.

or 10,000 nM) and wash (Figure 3F,G). To assess the specificity and accuracy of single-step protocol using **GC04-38**, fluorescent signals from PBMCs subjected to anti-DAT staining protocol were compared to the fluorescence signal detected in samples incubated with **GC04-38**. Consistent with previous reports, anti-DAT antibody staining reliably detected DAT with minimal background (Figure 3E), which was similar to the signal obtained in samples treated with fluorescent **GC04-38**, suggesting that **GC04-38**-bound DAT efficiently and specifically recognizes DAT in human PBMCs. Unlike DAT-expressing HEK cells, human monocytes and macrophages contain a large intercellular pool of DAT.[12] The dynamics of DAT trafficking to and away from the membrane has been studied extensively in multiple DAT expression cell types. Hypothetically, **GC04-38**-bound DAT is either membrane confined or traffics more slowly. Therefore, a longer incubation time or a higher concentration of **GC04-38** is predicted to produce an increasing fluorescent signal in a dose- or time-dependent manner. Since increasing incubation time will produce an infinite number of variables in live PBMCs (including cell death or phenotype change), we conducted a dose−response experiment in which PBMCs were incubated for 30 min on ice with 10 100, 1000, or 10,000 nM **GC04-38**. The 1000 nM concentration produced the most robust signal for DAT. There was no appreciable increase in DAT signal at 10,000 nM (Figure 3F,G), suggesting that 1000 nM is a saturating concentration.

Since a small subset of human PBMCs (∼4−5%) express NET, a parallel set of PBMCs were incubated with **GC04-38** in the presence of a NET blocker, desipramine (DMI) (Figure 3H). Compared to the fluorescent signal obtained in cells treated with **GC04-38** alone (Figure 3F), NET blockade (DMI pretreatment) produced a 3−5% decrease in **GC04-38** fluorescent signal (Figure 3G), which is consistent with recent reports[9,12] showing a small percentage of circulating PBMCs expressing NET.[9,12] To further assess the specificity of **GC04-38** for DAT, an additional set of PBMCs were incubated in parallel with both DMI and 100 mM JJC8-087, the nonfluorescent parent compound (Figure 1B,C) of **GC04-38**. Consistent with data shown in the rat striatal tissue (Table 1), the JJC8-087 pretreatment abolished the fluorescent **GC04-38** signal in PBMCs (Figure 3H,J). Taken together, these data suggest that **GC04-38** reliably detects DAT in human PBMCs. Importantly, the use of **GC04-38** not only detects surface DAT but also eliminates multiple limitations of immunostaining using primary and secondary antibodies to detect DAT, including fixation and permeabilization, providing a rapid and high-throughput

https://doi.org/10.1021/jacsau.3c00719
JACS Au 2024, 4, 657−665

method to detect surface DAT expression on circulating immune cells.

GC04-38 Labels DAT-Expressing Peripheral Immune Cells in Mice with a High Degree of Specificity

To confirm the specificity of **GC04-38** in detecting DAT-expressing PBMCs, we conducted parallel experiments in the PBMC of wild-type mice (C57/B6 mice) and mice with DAT gene deletion (DAT KO-C57/B6 background). To maintain uniformity comparing human and mouse data, we used a similar experimental design as described in Figure 4A, comparing the multistep antibody labeling (including fixation, permeabilization, and primary and secondary antibodies) with single-step **GC04-38** labeling. PBMCs isolated from whole blood were stained either fixed, permeabilized, and stained with anti-DAT antibody and species-specific secondary antibody, or PBMCs were stained with **GC04-38** (1000 nM) in the presence of DMI (Figure 4A–C). After debris exclusion, immunostaining for DAT reliably quantified DAT+ PBMCs in WT mice but not DAT KO mice (Figure 4E,F). Likewise, **GC04-38** detected a similar percentage of DAT+ PBMCs via flow cytometry in WT but not DAT KO mice, indicating that **GC04-38** is specific for DAT in PBMCs (Figure 4G,H). These data are also consistent with results obtained via the radioligand binding assay in Sprague–Dawley rat brain membranes (Table 1).

CONCLUSIONS

Flow cytometry has been the primarily used technology to study cell markers in suspension. We previously developed a flow cytometry method to accurately detect DAT in PBMCs.[25] Although this method is highly precise, it requires a multistep protocol that includes permeabilization, a series of washes in between incubations with a DAT antibody, and a fluorescent secondary antibody, limiting its utility as a high-throughput assay. Specifically, one of the significant drawbacks of conventional flow cytometry assays is the need for species-specific antibodies, such as human anti-DAT antibody, mouse anti-DAT antibody, and relevant secondary antibodies. These antibodies are not only expensive but also subject to considerable batch variability, which can affect the reproducibility of results across different laboratories using different sources or batches of the antibody. Most importantly, the validated DAT antibodies target the intracellular DAT domain, making it impossible to distinguish between surface and intracellular DAT pools. The fluorophore sulfo-Cy5 in **GC04-38** is cell impermeable and thus only binds surface DAT, overcoming the limitation of DAT antibodies that require a permeabilization step to reliably target membrane-bound DAT. Additionally, DAT-specific fluorescent probe application eliminates the need for cell fixation and permeabilization steps, thereby increasing the efficiency of cell sorting for transcriptomic studies, immunophenotyping, and other in vitro characterization.

Herein, we have described a novel and versatile fluorescently labeled ligand, based on our previously reported SAR campaign that yielded DAT-selective small molecules. We repurposed their utility by incorporating a fluorophore motif that ultimately afforded an unprecedented DAT-selective FLL. Finally, a highly promising feature of this probe includes the ability for fast detection of DAT in a single step from distinct species (e.g., human and mouse) and the elimination of previously required antibodies. This represents an outstanding characteristic for future reverse translational experimental strategy, providing a platform to advance our fundamental understanding of DAT expression and activity more rapidly in PBMCs in health and disease and its potential as a peripheral biomarker.

METHODS

Detailed synthetic schemes, experimental procedures, and general information regarding analytical instrumentation can be found in the Supporting Information (SI), including NMR and HRMS spectra. Radioligand binding assay and flow cytometry protocols are also detailed in the SI.

ASSOCIATED CONTENT

Supporting Information

The Supporting Information is available free of charge at https://pubs.acs.org/doi/10.1021/jacsau.3c00719.

General information; synthetic schemes, procedures, and characterization; radioligand binding assay method; human subjects; HEK293T culture and isolation; PBMC isolation; flow cytometry; JHC1-64 labels DAT-expressing cells via microscopy but not by flow cytometry; NMR spectra; and HRMS (PDF)

AUTHOR INFORMATION

Corresponding Author

Amy Hauck Newman − *Medicinal Chemistry Section, Molecular Targets and Medications Discovery Branch, National Institute on Drug Abuse − Intramural Research Program, National Institutes of Health, Baltimore, Maryland 21224, United States;* orcid.org/0000-0001-9065-4072; Phone: (410) 952-0410; Email: anewman@intra.nida.nih.gov

Authors

Gisela Andrea Camacho-Hernandez − *Medicinal Chemistry Section, Molecular Targets and Medications Discovery Branch, National Institute on Drug Abuse − Intramural Research Program, National Institutes of Health, Baltimore, Maryland 21224, United States*

Adithya Gopinath − *Department of Neuroscience, University of Florida College of Medicine, Gainesville, Florida 32611, United States*

Amarachi V. Okorom − *Medicinal Chemistry Section, Molecular Targets and Medications Discovery Branch, National Institute on Drug Abuse − Intramural Research Program, National Institutes of Health, Baltimore, Maryland 21224, United States*

Habibeh Khoshbouei − *Department of Neuroscience, University of Florida College of Medicine, Gainesville, Florida 32611, United States*

Complete contact information is available at: https://pubs.acs.org/10.1021/jacsau.3c00719

Author Contributions

G.A.C.-H., A.G., H.K., and A.H.N. conceived the study. G.A.C.-H., A.G., H.K. and A.H.N. wrote the manuscript with input of all authors; G.A. C.-H., A.G., H.K., and A.H.N. designed and/or supervised the experiments and data analyses; G.A.C.-H., and A.V.O. performed the synthesis and the radioligand binding experiments. A.G. performed the flow cytometry experiments.

Funding

Funding for this work was provided by the National Institute on Drug Abuse-Intramural Research Program (Z1A DA000389 to

A.H.N.), National Institute on Drug Abuse (R01DA058143-01 to H.K.), National Institute of Neurological Disorders and Stroke (R01NS071122-07, R21NS133384-01, and R01DA058143-01 to H.K.), the Evelyn F. and William L. McKnight Brain Institute's Gator NeuroScholar's program (to A.G.), and the Karen Toffler Charitable Trust (to A.G.).

Notes

The authors declare no competing financial interest.

■ ACKNOWLEDGMENTS

These studies were accomplished using instrumentation and technical assistance from the University of Florida Center for Immunology and Transplantation. The authors thank Dr. Shelley Jackson [NIDA-IRP Translational Analytical Core (TAC)] for the high-resolution mass spectrometry analyses; Dr. Laura Kozell and Dr. Aaron Janowsky [Oregon Health & Science University (OHSU)] for providing the hDAT-HEK 293 cell line and their assistance with culture protocols; Dr. Ning Sheng Cai (NIDA-IRP Integrative Neurobiology Section) for assistance with tissue culture protocols; and Dr. Alessandro Bonifazi and Dr. Khorshada Jahan (NIDA-IRP Medicinal Chemistry Section) for constructive edits to the SI. Figures were created with BioRender.com under a premium license.

■ REFERENCES

(1) Klein, M. O.; Battagello, D. S.; Cardoso, A. R.; Hauser, D. N.; Bittencourt, J. C.; Correa, R. G. Dopamine: Functions, Signaling, and Association with Neurological Diseases. *Cell Mol. Neurobiol* **2019**, *39* (1), 31−59.

(2) Gopinath, A.; Mackie, P. M.; Phan, L. T.; Tansey, M. G.; Khoshbouei, H. The complex role of inflammation and gliotransmitters in Parkinson's disease. *Neurobiol Dis* **2023**, *176*, No. 105940.

(3) Mackie, P.; Lebowitz, J.; Saadatpour, L.; Nickoloff, E.; Gaskill, P.; Khoshbouei, H. The dopamine transporter: An unrecognized nexus for dysfunctional peripheral immunity and signaling in Parkinson's Disease. *Brain Behav Immun* **2018**, *70*, 21−35.

(4) Gether, U.; Andersen, P. H.; Larsson, O. M.; Schousboe, A. Neurotransmitter transporters: molecular function of important drug targets. *Trends Pharmacol. Sci.* **2006**, *27* (7), 375−383.

(5) Kristensen, A. S.; Andersen, J.; Jorgensen, T. N.; Sorensen, L.; Eriksen, J.; Loland, C. J.; Stromgaard, K.; Gether, U. SLC6 neurotransmitter transporters: structure, function, and regulation. *Pharmacol Rev.* **2011**, *63* (3), 585−640.

(6) Ben-Shaanan, T. L.; Azulay-Debby, H.; Dubovik, T.; Starosvetsky, E.; Korin, B.; Schiller, M.; Green, N. L.; Admon, Y.; Hakim, F.; Shen-Orr, S. S.; et al. Activation of the reward system boosts innate and adaptive immunity. *Nat. Med.* **2016**, *22* (8), 940−944.

(7) Ben-Shaanan, T. L.; Schiller, M.; Azulay-Debby, H.; Korin, B.; Boshnak, N.; Koren, T.; Krot, M.; Shakya, J.; Rahat, M. A.; Hakim, F.; et al. Modulation of anti-tumor immunity by the brain's reward system. *Nat. Commun.* **2018**, *9* (1), 2723.

(8) Koren, T.; Yifa, R.; Amer, M.; Krot, M.; Boshnak, N.; Ben-Shaanan, T. L.; Azulay-Debby, H.; Zalayat, I.; Avishai, E.; Hajjo, H.; et al. Insular cortex neurons encode and retrieve specific immune responses. *Cell* **2021**, *184* (24), 5902−5915.e17.

(9) Gopinath, A.; Mackie, P.; Hashimi, B.; Buchanan, A. M.; Smith, A. R.; Bouchard, R.; Shaw, G.; Badov, M.; Saadatpour, L.; Gittis, A.; et al. DAT and TH expression marks human Parkinson's disease in peripheral immune cells. *NPJ. Parkinsons Dis* **2022**, *8* (1), 72.

(10) Gopinath, A.; Mackie, P. M.; Phan, L. T.; Mirabel, R.; Smith, A. R.; Miller, E.; Franks, S.; Syed, O.; Riaz, T.; Law, B. K.; et al. Who Knew? Dopamine Transporter Activity Is Critical in Innate and Adaptive Immune Responses. *Cells* **2023**, *12* (2), 269.

(11) Gopinath, A.; Riaz, T.; Miller, E.; Phan, L.; Smith, A.; Syed, O.; Franks, S.; Martinez, L. R.; Khoshbouei, H. Methamphetamine induces a low dopamine transporter expressing state without altering the total number of peripheral immune cells. *Basic Clin. Pharmacol. Toxicol.* **2023**, *133*, 496.

(12) Mackie, P. M.; Gopinath, A.; Montas, D. M.; Nielsen, A.; Smith, A.; Nolan, R. A.; Runner, K.; Matt, S. M.; McNamee, J.; Riklan, J. E.; et al. Functional characterization of the biogenic amine transporters on human macrophages. *JCI Insight* **2022**, *7* (4), No. e151892, DOI: 10.1172/jci.insight.151892.

(13) Eriksen, J.; Rasmussen, S. G.; Rasmussen, T. N.; Vaegter, C. B.; Cha, J. H.; Zou, M. F.; Newman, A. H.; Gether, U. Visualization of dopamine transporter trafficking in live neurons by use of fluorescent cocaine analogs. *J. Neurosci.* **2009**, *29* (21), 6794−6808.

(14) Dekkers, S.; Caspar, B.; Goulding, J.; Kindon, N. D.; Kilpatrick, L. E.; Stoddart, L. A.; Briddon, S. J.; Kellam, B.; Hill, S. J.; Stocks, M. J. Small-Molecule Fluorescent Ligands for the CXCR4 Chemokine Receptor. *J. Med. Chem.* **2023**, *66*, 5208.

(15) Guthrie, D. A.; Klein Herenbrink, C.; Lycas, M. D.; Ku, T.; Bonifazi, A.; DeVree, B. T.; Mathiasen, S.; Javitch, J. A.; Grimm, J. B.; Lavis, L.; et al. Novel Fluorescent Ligands Enable Single-Molecule Localization Microscopy of the Dopamine Transporter. *ACS Chem. Neurosci.* **2020**, *11* (20), 3288−3300.

(16) Vernall, A. J.; Hill, S. J.; Kellam, B. The evolving small-molecule fluorescent-conjugate toolbox for Class A GPCRs. *Br. J. Pharmacol.* **2014**, *171* (5), 1073−1084.

(17) Toy, L.; Huber, M. E.; Schmidt, M. F.; Weikert, D.; Schiedel, M. Fluorescent Ligands Targeting the Intracellular Allosteric Binding Site of the Chemokine Receptor CCR2. *ACS Chem. Biol.* **2022**, *17* (8), 2142−2152.

(18) Camacho-Hernandez, G. A.; Jahan, K.; Newman, A. H. Illuminating the monoamine transporters: Fluorescently labelled ligands to study dopamine, serotonin and norepinephrine transporters. *Basic Clin. Pharmacol. Toxicol.* **2023**, *133*, 473.

(19) Cha, J. H.; Zou, M. F.; Adkins, E. M.; Rasmussen, S. G.; Loland, C. J.; Schoenenberger, B.; Gether, U.; Newman, A. H. Rhodamine-labeled 2beta-carbomethoxy-3beta-(3,4-dichlorophenyl)tropane analogues as high-affinity fluorescent probes for the dopamine transporter. *J. Med. Chem.* **2005**, *48* (24), 7513−7516.

(20) Lycas, M. D.; Ejdrup, A. L.; Sorensen, A. T.; Haahr, N. O.; Jorgensen, S. H.; Guthrie, D. A.; Stoier, J. F.; Werner, C.; Newman, A. H.; Sauer, M.; et al. Nanoscopic dopamine transporter distribution and conformation are inversely regulated by excitatory drive and D2 autoreceptor activity. *Cell Rep* **2022**, *40* (13), No. 111431.

(21) Kumar, V.; Rahbek-Clemmensen, T.; Billesbolle, C. B.; Jorgensen, T. N.; Gether, U.; Newman, A. H. Novel and high affinity fluorescent ligands for the serotonin transporter based on (s)-citalopram. *ACS Med. Chem. Lett.* **2014**, *5* (6), 696−699.

(22) Camacho-Hernandez, G. A.; Casiraghi, A.; Rudin, D.; Luethi, D.; Ku, T. C.; Guthrie, D. A.; Straniero, V.; Valoti, E.; Schutz, G. J.; Sitte, H. H.; et al. Illuminating the norepinephrine transporter: fluorescent probes based on nisoxetine and talopram. *RSC Med. Chem.* **2021**, *12* (7), 1174−1186.

(23) Luethi, D.; Maier, J.; Rudin, D.; Szollosi, D.; Angenoorth, T. J. F.; Stankovic, S.; Schittmayer, M.; Burger, I.; Yang, J. W.; Jaentsch, K.; et al. Phosphatidylinositol 4,5-bisphosphate (PIP2) facilitates norepinephrine transporter dimerization and modulates substrate efflux. *Commun. Biol.* **2022**, *5* (1), 1259.

(24) Cao, J.; Slack, R. D.; Bakare, O. M.; Burzynski, C.; Rais, R.; Slusher, B. S.; Kopajtic, T.; Bonifazi, A.; Ellenberger, M. P.; Yano, H.; et al. Novel and High Affinity 2-[(Diphenylmethyl)sulfinyl]acetamide (Modafinil) Analogues as Atypical Dopamine Transporter Inhibitors. *J. Med. Chem.* **2016**, *59* (23), 10676−10691.

(25) Gopinath, A.; Doty, A.; Mackie, P. M.; Hashimi, B.; Francis, M.; Saadatpour, L.; Saha, K.; Shaw, G.; Ramirez-Zamora, A.; Okun, M. S.; et al. A novel approach to study markers of dopamine signaling in peripheral immune cells. *J. Immunol Methods* **2020**, *476*, No. 112686.

(26) Slack, R. D.; Ku, T. C.; Cao, J.; Giancola, J. B.; Bonifazi, A.; Loland, C. J.; Gadiano, A.; Lam, J.; Rais, R.; Slusher, B. S.; et al. Structure-Activity Relationships for a Series of (Bis(4-fluorophenyl)-methyl)sulfinyl Alkyl Alicyclic Amines at the Dopamine Transporter:

Functionalizing the Terminal Nitrogen Affects Affinity, Selectivity, and Metabolic Stability. *J. Med. Chem.* **2020**, *63* (5), 2343−2357.
(27) Deo, C.; Abdelfattah, A. S.; Bhargava, H. K.; Berro, A. J.; Falco, N.; Farrants, H.; Moeyaert, B.; Chupanova, M.; Lavis, L. D.; Schreiter, E. R. The HaloTag as a general scaffold for far-red tunable chemigenetic indicators. *Nat. Chem. Biol.* **2021**, *17* (6), 718−723.
(28) Gaskill, P. J.; Carvallo, L.; Eugenin, E. A.; Berman, J. W. Characterization and function of the human macrophage dopaminergic system: implications for CNS disease and drug abuse. *J. Neuroinflammation* **2012**, *9*, 203.
(29) Matt, S. M.; Gaskill, P. J. Where Is Dopamine and how do Immune Cells See it?: Dopamine-Mediated Immune Cell Function in Health and Disease. *J. Neuroimmune Pharmacol* **2020**, *15* (1), 114−164.
(30) Ciliax, B. J.; Heilman, C.; Demchyshyn, L. L.; Pristupa, Z. B.; Ince, E.; Hersch, S. M.; Niznik, H. B.; Levey, A. I. The dopamine transporter: immunochemical characterization and localization in brain. *J. Neurosci.* **1995**, *15* (3), 1714−1723.

https://doi.org/10.1021/jacsau.3c00719
JACS Au 2024, 4, 657−665